Research Square

Preprints are preliminary reports that have not undergone peer review.
They should not be considered conclusive, used to inform clinical practice,
or referenced by the media as validated information.

Carbonic anhydrase activity carriers and their differential sensitivity to heavy metals in Chenopodium album leaves

Elena K. Zolotareva

e.zolotareva@ukr.net

M.G. Kholodny Institute of Botany

Nataliia M. Topchiy

M.G. Kholodny Institute of Botany

Olena B. Onoiko

M.G. Kholodny Institute of Botany

Research Article

Keywords: leaf proteins, enzyme inhibition, heavy metals, protonography, Rubisco depletion, biomarkers

Posted Date: November 25th, 2026

DOI: https://doi.org/10.21203/rs.3.rs-11606515/v1

License: This work is licensed under a Creative Commons Attribution 4.0 International License.
Read Full License

Additional Declarations: No competing interests reported.

Carbonic anhydrase activity carriers and their differential sensitivity to heavy metals in *Chenopodium album* leaves

Elena K. Zolotareva, Nataliia M. Topchiy, Olena B. Onoiko

https://orcid.org/0000-0001-7399-2213
https://orcid.org/0000-0003-4694-5707
https://orcid.org/0000-0003-4902-0937

M.G. Kholodny Institute of Botany, Natl. Acad. Sci. Ukraine, Tereshchenkivs'ka St.,2 Kyiv, 01004, Ukraine, E-mail: inst@botany.kiev.ua

Corresponding author: Elena K. Zolotareva – E-mail: e.zolotareva@ukr.net;

tel: +380985320363

Elena K. Zolotareva – e.zolotareva@ukr.net

Nataliia M. Topchiy – ntopchiy@ukr.net

Olena B. Onoiko – elena_onoiko@ukr.net

Abstract

Carbonic anhydrase (CA; EC 4.2.1.1) provides CO_2 supply for photosynthesis and metabolism. CA is a metal-containing enzyme that may be sensitive to environmental contaminants, but its biochemical profile and metal-response characteristics in many non-model plant species remain poorly characterized. Here, we developed a two-stage ethanol-fractionation procedure to enrich soluble CA activity from *Chenopodium album* L. leaves and examined the associated activity carriers and their responses to selected heavy-metal ions. The post-ethanol fraction showed an approximately 11-fold increase in CA-specific activity compared with the crude extract, although total CA activity decreased during fractionation, indicating incomplete recovery. Electrophoretic analysis and protonography revealed five CA activity carriers with apparent molecular masses of approximately 26, 36, 44, 52, and 62 kDa. The 26- and 52-kDa bands also exhibited esterase activity, whereas the inhibitor-response data were consistent with the presence of acetazolamide-sensitive plant CA activities. In concentration–response experiments, Hg^{2+} and Ag^{+} were the strongest inhibitors, with estimated IC_{50} values of approximately 0.28 and 0.35 μM, respectively. Cd^{2+} and Cu^{2+} produced moderate inhibition, Zn^{2+} was weakly inhibitory, and Pb^{2+} had little effect under the assay conditions. The marked sensitivity to Hg^{2+} and Ag^{+} may involve interactions with protein thiol groups, although this mechanism was not directly tested. These results provide a biochemical profile of CA-associated activity in *C. album* and demonstrate differential sensitivity to heavy-metal ions. CA activity may therefore represent a promising candidate biochemical indicator of exposure to selected metals; however, validation using metal-exposed plants, tissue-metal measurements, and field samples is required.

Keywords: leaf proteins; enzyme inhibition; heavy metals; protonography; Rubisco depletion; biomarkers

1. Introduction

1. Introduction

Carbonic anhydrases (CA; EC 4.2.1.1) are metalloproteins that catalyze the reversible hydration of carbon dioxide to form bicarbonate and protons:

$$CO_2 + H_2O \rightleftharpoons HCO_3^- + H^+$$

This simple, reversible reaction is of immense importance for plant cell metabolism, since it allows gaseous carbon dioxide to be incorporated into carbon fixation and transformation in

the liquid phase of plant cells. However, spontaneous CO_2 hydration is too slow to sustain the rapid inorganic carbon fluxes required for metabolism and photosynthesis (Swenson and Maren 1978; Occhipinti and Boron 2019). To overcome this physiological bottleneck, organisms have evolved multiple forms of CA that differ in their catalytic properties, cellular localization, regulation, and sensitivity to environmental conditions. These enzymes are widespread across living organisms and are represented by several unrelated families, including α-, β-, γ-, δ-, ζ-, η-, θ-, and ι-CAs. This indicates that convergent evolution toward this essential catalytic function also reflects repeated adaptation to different ecological and biochemical contexts (DiMario et al. 2017; Supuran 2016; 2025; Momayyezi et al. 2020).

Higher plants express members of the α-, β-, and γ-carbonic anhydrase families across a wide variety of tissues and cellular compartments (DiMario et al. 2017; Momayyezi et al. 2020). Encoded by numerous genes (Fabre et al. 2007, Momayyezi et al. 2020), the resulting isoforms vary significantly in their amino acid sequences, three-dimensional architectures, oligomeric organizations, and active-site metal coordination. Numerous CA genes and isoforms are expressed in various tissues and localized in several cellular compartments. (Fabre et al. 2007; Momayyezi et al. 2020).

The most widespread and well-studied class of plant carbonic is β-type enzymes. γ-CAs are mainly associated with the CA-domain of mitochondrial complex I. α-CAs remain relatively poorly understood in terms of their localization and physiological functions (Langella et al. 2022). Soluble CAs, localized in the chloroplast stroma and cytosol of C3 plant leaves, are predominantly represented of the β-type. They typically function as dimers, tetramers, or higher oligomers in photosynthetic tissues (Kimber and Pai 2000).

CAs participate in many metabolic functions that involve carboxylation or decarboxylation reactions, including both photosynthesis and respiration. They facilitate the rapid equilibration of CO_2 and HCO_3^-, influencing the CO_2 supply to RuBisCo (Igamberdiev 2015) and providing bicarbonate for anabolic pathways, including nucleotide, fatty acid, and amino acid biosynthesis (Hoang and Chapman 2002; Moroney 2026). Furthermore, leaf CAs may integrate the photosynthetic carbon cycle with nitrate assimilation, organic acid metabolism, and stomatal responses (Hines et al. 2021; Hu et al.2015). Notably, chloroplast β-CA is extremely abundant, often considered second only to RuBisCo in leaf soluble protein content (Occhipinti and Boron 2019; Okabe et al. 1984; Peltier et al. 2006).

Studying the effects of heavy metals is important for gaining insight into the catalytic mechanisms of enzymes and their physiological vulnerability under environmental stress. Enzymes are valuable biomarkers for assessing organismal responses to HM exposure because

they catalyze virtually all biochemical reactions in living systems (Chibuike and Obiora 2014). This sensitivity makes enzymes particularly useful for detecting early-stage environmental contamination before overt biological damage is apparent (Rao et al. 2014; González-González et al. 2022). The inhibitory effect of metals on carbonic anhydrases in animals has been studied in great detail (Lionetto et al. 2012; 2016), which confirmed the possibility of using carbonic anhydrases in bioindication of environmental pollution (Caricato et al. 2014; Lionetto et al. 2019). To date, there is only limited information on the impact of HMs on plant carbon anhydrases, and this is restricted to a small number of species (Asencio and Cedeno-Maldonado 1978; Rowlett et al. 1994; Polishchuk et al. 2018; Zolotareva et al. 2025). Such studies could be particularly valuable for non-model plant species, especially those that can grow in contaminated soils.

The subject of this study is *Chenopodium album* L. (common lambsquarters), a highly adaptive, fast-growing annual weed belonging to the Amaranthaceae family. This species possesses an exceptional capacity for colonizing new territories and thrives across a wide range of geographical and ecological conditions, including heavily contaminated sites (Li and Watkinson, 2000; Aloud et al., 2023). In addition to its tolerance to elevated concentrations of heavy metals (HMs), *C. album* is capable of efficiently accumulating elements such as cadmium (Cd), chromium (Cr), copper (Cu), nickel (Ni), lead (Pb), and zinc (Zn), making it a promising candidate for phytoremediation and biomonitoring (Gupta and Sinha, 2007; Mohan et al., 2019; Sharma et al., 2020; Tőzsér et al., 2019; Ugulu et al., 2022; Flores-Calla et al., 2024).

In this study, we measured total CA activity and identified distinct CA forms in the soluble protein fraction of *C. album* leaves for the first time. We also examined the effects of selected metal ions (Zn^{2+}, Cd^{2+}, Cu^{2+}, Hg^{2+}, and Ag^{+}) on total CA activity. These results will make it possible to evaluate the relative sensitivity of total CA activity to heavy metal ions in *C. album* leaves.

2. Materials and methods

2.1. Plant material

Seeds/plant material of Chenopodium album L. (Amaranthaceae s.l. / Chenopodiaceae s. str.) was collected in in autumn 2022 from wild populations growing in uninhabited areas of the Feofania Park, in the southern part of the City of Kyiv, Ukraine (GPS coordinates are approximately 50.3405° N, 30.4889° E). Since the *C.album* aggregate is a taxonomically complicated group that in the study area includes diploids and allopolyploids (tetraploids and hexaploids) (see Mosyakin and Mandák 2020; Habibi et al. 2023; Mandák et al. 2025, and references therein), the precise identification of the plant material was of utmost importance.

Voucher specimens of the material are deposited in the publicly available herbarium collection, the National Herbarium of Ukraine [KW, the international acronym according to Index Herbariorum 2026 (updated continuously)] at the M.G. Kholodny Institute of Botany. *C. album* is a widespread, and non-protected ruderal weedy species, and because of that no specific permits were or are required for its collection in public/unprotected areas in Ukraine and in most of the countries of the world. Mature seeds of *Chenopodium album* L. were collected from plants in Feofaniya Nature Park (Kyiv, Ukraine) in autumn 2022 All experimental research actions on this plant material, including its collection and further treatment, were conducted in full compliance with the relevant institutional, national, and international guidelines and legislation, including the IUCN Policy Statement on Research Involving Species at Risk of Extinction and the Convention on the Trade in Endangered Species of Wild Fauna and Flora.

The seeds were sown evenly at a depth of 1–2 cm in pots filled with ready-to-use all-purpose potting soil for houseplants ("Eco Plus," Ukraine) and placed in direct sunlight near glass windows at a temperature of 22–29 °C. During germination, pots were watered from above with settling tap water to maintain soil moisture at approximately 70% of field capacity. Leaves of C. album were harvested 20 days after sowing.

2.2. Extraction of soluble leaf proteins

The isolation of the soluble leaf protein fraction was carried out by the methods of Pocker and Ng (1973) or Makino et al. (1992). The Bradford method (1976) was used to control the protein content in fractions.

2.3. Protein precipitation by ethanol

Soluble proteins were precipitated from the crude leaf extract using ethanol according to the protocol described by Matulis (2016). The crude extract (volume V_0) was mixed with 0.45 V_0 of ethanol pre-cooled to 4 °C, resulting in a final ethanol concentration of 30% (v/v). The mixture was centrifuged at 5000 × g for 10 min at 4 °C, after which the precipitate was discarded. Subsequently, six volumes of pre-chilled ethanol were added to one volume of the supernatant to obtain a final ethanol concentration of 90% (v/v). Protein precipitation was completed within 1–1.5 h at 4 °C.

The upper, transparent, ethanol-containing phase was carefully removed by siphoning, and the remaining lower phase was centrifuged at 10,000 × g for 10 min at 4 °C. The resulting pellet was air-dried and residual ethanol was removed using a stream of nitrogen gas. The pellet was then resuspended in Tris–HCl buffer (0.0125 M, pH 6.8). Insoluble material was

removed by centrifugation, and protein concentration and carbonic anhydrase (CA) activity were determined in the resulting supernatant.

2.4. Determination of CA activity in the leaf protein fraction

The hydratase activity of carbonic anhydrase (CA) was determined by measuring the pH change resulting from the enzyme-catalyzed conversion of CO_2 to bicarbonate, following Capasso et al. (2012). Assays were performed at 0 °C in glass tubes immersed in an ice–water bath. To each tube were added 0.5 mL of 25 mM Tris–SO_4 buffer, bromothymol blue (BTB) as pH indicator, and an aliquot of the protein fraction corresponding to 10 μg of protein. The reaction was initiated by rapidly adding 0.5 mL of ice-cold water saturated with CO_2 and simultaneously starting a stopwatch. The time required for the indicator color to change from blue to yellow (corresponding to the pH drop) was recorded. Enzyme activity was expressed in Wilbur–Anderson units (WAU) and calculated as (T0 − T)/T, where T0 and T are the times (s) for the pH decrease (from pH 8.3 to the indicator transition point) in the uncatalyzed control and in the presence of enzyme, respectively. Activity is reported as units per mg protein.

2.5. Electrophoretic analysis

Native polyacrylamide gel electrophoresis (PAGE) of soluble leaf proteins was performed using a Mini-PROTEAN Tetra Cell system (Bio-Rad) according to Ornstein and Davis (1964). The stacking (focusing) gel contained 4% acrylamide in 0.0625 M Tris–HCl (pH 6.8), and the resolving gel contained 7% acrylamide in 0.375 M Tris–HCl (pH 8.8). Electrophoresis was carried out at 75 mA and 0 °C for 1 h. 20 μg of protein were loaded per well.

Protonography of soluble *C. album* leaf proteins was performed as described by De Luca et al. (2015). SDS–PAGE was carried out under nonreducing conditions (no 2-mercaptoethanol and no boiling) following Laemmli (1970) in 12% resolving gels prepared in 0.375 M Tris–HCl (pH 8.8). The stacking gel contained 4% acrylamide in 0.125 M Tris–HCl (pH 6.8). The running buffer was Tris–glycine (25 mM Tris–HCl, 192 mM glycine), and 0.1% (w/v) SDS was included in the resolving gel and the upper running buffer. 20 μg of protein were loaded per well. Protein Marker III (6.5–200 kDa; PanReac Applichem) was used as molecular-mass standards.

After electrophoresis, selected gels were stained with Coomassie Brilliant Blue R-250. Other gels were incubated in 2.5% (v/v) Triton X-100 for 1 h on a shaker to remove SDS and

recover SDS-inhibited hydratase activity, then washed twice for 10 min in 100 mM Tris–HCl (pH 8.2) containing 10% isopropanol.

2.6. Visualization of the CA activity in PAAG

Visualization of the hydratase activity in gels by production of protons (H^+) in the reaction of CO_2 hydration was carried out according to Edwards and Patton (1966). The gels were incubated for 30 min at 0°C in 44 mM veronal buffer (pH 8.1) with the addition of a pH-indicator, 0.2% BTB, until the gel turns dark blue. Then the gel was transferred to water saturated with CO_2 at 0° C. A local decrease in pH in the protein zones exhibiting CA activity was evidenced by the formation of yellow bands due to a change in the color of the indicator from blue (alkaline pH) to yellow (acidic pH).

2.7. Visualization of the esterase activity in PAAG

Esterase activity of CA in gels was determined according to Kumar et.al. (2019; 2022) After the electrophoresis the gels were incubated overnight in 0.1 M Tris-HC1 buffer (pH 7.4) containing the ester substrate β-Naphthyl acetate (75 μM in ethanol) and azo dye Fast-Blue-BB (0.12% in ethanol). The liberated β-Naphthol reacted with FB-BB to give a violet color in regions with esterase activity.

AI-driven image processing was used to improve contrast and band differentiation in electrophoretic gel images after the visualization of CA and esterase activities. Adjustments were applied uniformly across the entire image and that original uncropped scans are provided in the supplementary file.

2.8. *Treatment of protein samples with HM salts*

Because CA activity is measured at 0 °C in an ice–water bath (Capasso et al. 2012), preliminary experiments revealed that not all metals inhibit CA activity under these conditions when added directly to the reaction cell. Therefore, prior to measuring CA activity, aliquots of the enzyme were incubated in the presence of each test concentration of HM at room temperature. The incubation time required to achieve a specific level of inhibition depended on the nature of the HM. For Ag^+ or Hg^{2+} to exhibit an inhibitory effect, no more than 1 min was required, whereas the effect of Pb developed over more than 4 min. To standardize the conditions for generating dose–response curves of CA activity as a function of HM ion concentration, all samples were pre-incubated with the tested HM concentrations for 5 min at room temperature prior to activity measurements. Control activity in the absence of the inhibitor

was taken as 100%. IC_{50} values were determined by nonlinear regression using a four-parameter logistic model (variable slope) of log(inhibitor) concentration versus response.

IC_{50} values were determined by nonlinear regression using a four-parameter logistic model (variable slope) of log(inhibitor) concentration versus response. Curve fitting was performed using GraphPad Prism (version 9.0.1). The IC_{50} values are reported as a best-fit estimates.

The samples for electrophoretic analysis were prepared based on the following ratios of HM to protein (nmol/μg protein): 0.01–0.04 for $AgNO_3$ and 0.05–0.15 for $CdCl_2$. All samples were pre-incubated with HM salts for 10 min before the loading to the gel.

2.9. Statistical analysis

The results were displayed as mean values of at least five independent experiments. All measurements of CA rates were performed in triplicate. Student's t-test was used to compare the samples, the differences were considered reliable at $p < 0.05$.

3. Results

3.1. Partial purification and concentration carbonic anhydrase from C.album leaves using ethanol fractionation

Previous studies have shown that *Chenopodium album* leaves contain between 3.7% and 5% protein (Poonia and Upadhayay, 2015), which is approximately twice the protein content found in common leafy vegetables such as spinach and kale. However, using the protein extraction method described by Makino et al. (1992), we extracted a significantly lower amount of protein (<1%) (Table 1). Figure 1 shows the electrophoretic analysis of the extracted proteins using 7% polyacrylamide gel electrophoresis (PAGE) under non-denaturing conditions. The extracted proteins resolved into three distinct bands. The mobility of the most intense band corresponds to an apparent molecular mass of approximately 476 kDa. Additionally, there is a clearly distinguishable high-molecular-mass band corresponding to approximately 900 kDa, and a less intense band corresponding to approximately 239 kDa.

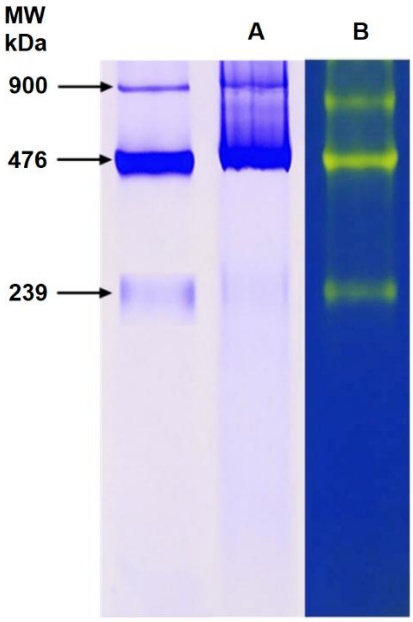


Figure 1. Non-denaturing PAGE of soluble proteins from a crude extract of *Chenopodium album* leaves. Gels were stained with Coomassie Brilliant Blue (lane A) or with bromothymol blue (BTB) to visualise carbonic anhydrase (CA) activity (lane B). The soluble protein fraction was isolated according to the method of Pocker and Ng (1973). Molecular mass markers included horse spleen ferritin dimer (900 kDa) and monomer (476 kDa), and catalase (239 kDa). Full-length, uncropped original gels are presented in Supplementary File 1.

Carbonic anhydrase (CA) activity in the 7% native gel was primarily detected in poorly resolved, diffuse areas within the high-molecular-mass region. This suggests that, in their native state, carbonic anhydrases associate with other proteins to form multienzyme complexes, a phenomenon extensively reported in previous literature (Suss et al. 1993; Jebanathirajah and Coleman 1998; Anderson and Carol 2004; Lazova and Stemler 2008: Gontero et al.2018; Zhang and Fernie, 2021).

To concentrate and partially purify carbonic anhydrases from *C. album* leaves, the soluble protein fraction was fractionated with ethanol as described in the Materials and Methods section. First, the total protein content and CA activity were determined in the crude leaf extract. The same analyses were then carried out on the water-soluble protein fraction obtained after ethanol precipitation and subsequent solubilization. The results are presented in Table 1.

Table 1.

The total protein content and carbonic anhydrase (CA) activity of the crude extract of *C. album* leaves, as well as the protein fraction obtained after ethanol precipitation

	Total protein content, mg	Total CA activity, WAU	Specific CA activity, WAU/mg protein

Extract 100 g of fresh leaves, according to Makino et al. (1992)	833	154908.77	185.96
Soluble protein fraction after two-stage ethanol precipitation	28.75	59617.24	2073.64

The total amount of water-soluble proteins in the leaf extract decreased nearly 29-fold following the two-stage ethanol precipitation, indicating that high ethanol concentrations irreversibly denature the majority of proteins extracted from *C. album* leaves. In contrast, a substantial portion of carbonic anhydrases (CAs) appear to undergo reversible precipitation, regaining their catalytic activity upon redissolution. However, the 2.5-fold decrease in total CA activity observed in the protein fraction obtained after precipitation (hereafter referred to as the post-ethanol fraction; Table 1) suggests that this recovery is not absolute. This loss of total activity is likely due to incomplete precipitation during the fractionation stages or partial irreversible denaturation. Despite this overall loss in total activity, the massive removal of other proteins resulted in an 11-fold increase in specific CA activity in the post-ethanol fraction (Table 1).

3.2. Electrophoretic analysis of post-ethanol fraction

Figure 2 presents a comparison of the native electrophoretic analyses of proteins from the crude leaf extract (lane A1) and the post-ethanol fraction (lanes A2 and A3). Equal amounts of protein (20 μg) were loaded into lanes A1 and A3, whereas half this amount (10 μg) was loaded into lane A2.

The number and intensity of protein bands in the post-ethanol fraction differed markedly from those observed in the crude extract (Figure 2A). The most intense band in lane A1 most likely corresponds to the most abundant leaf protein, ribulose-1,5-bisphosphate carboxylase/oxygenase (RuBisCo). This band (Rf = 0.29), along with bands at Rf = 0.18 and 0.32, was completely absent from the PAGE profiles of the post-ethanol fraction (lanes A2 and A3), indicating irreversible denaturation during exposure to high ethanol concentrations. In contrast, bands with Rf values of 0.21 and 0.47, which were detectable in the crude extract, exhibited substantially increased intensity in the electropherograms of the post-ethanol fraction (lanes A2 and A3). In addition, the post-ethanol fraction contained several polypeptides with Rf values of 0.64, 0.84, and 0.90 that were weakly detectable or absent in the crude extract.

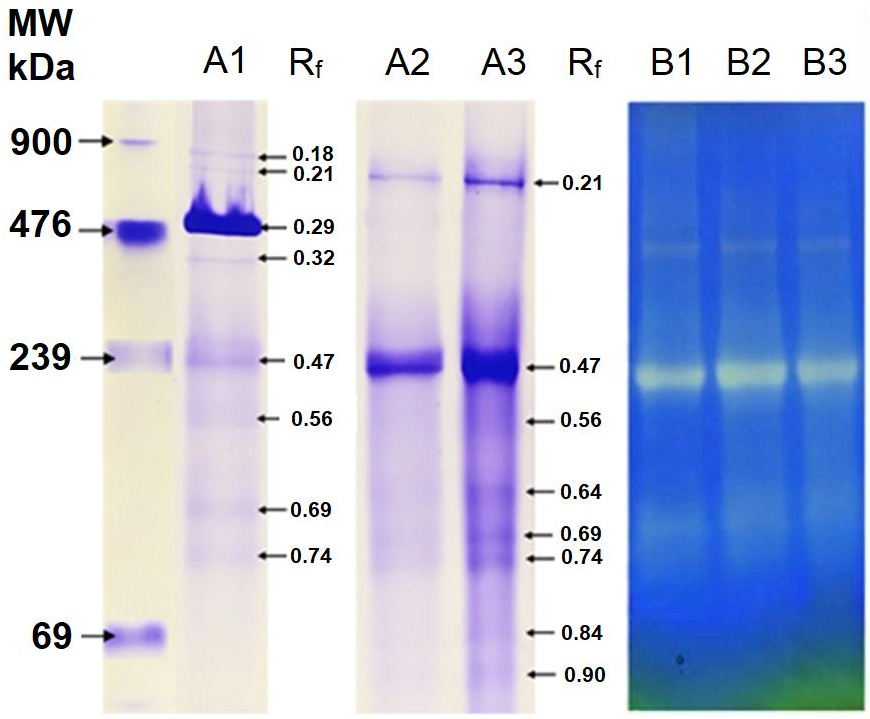


Figure 2. A comparative native PAGE of proteins of the crude leaf extract (lane A1) and the protein fraction obtained after ethanol fractionation (lanes A2 and A3). Lanes A1, A2 and A3 show Coomassie blue-stained soluble proteins extracted from *C. album* leaves, as described by Makino et al. (1992). Lanes B1, B2 and B3 show the visualization of CA activity in gels after BTB staining. Polypeptide bands and their CA activity were visualized sequentially in the same gel. Firstly, CA activity was detected for 5–10 min, after which the gels were photographed, thoroughly washed, and subsequently stained with Coomassie blue. The amount of protein loaded per well is as follows: A1 (B1) and A3 (B3): 20 µg; A2 (B2): 10 µg. The following proteins were used as markers: horse spleen ferritin dimer (900kDa), horse spleen ferritin monomer (476kDa), catalase (239kDa) and bovine serum albumin (69kDa). Full-length, uncropped original gels are presented in Supplementary File 1.

The visualization of CA activity revealed markedly higher activity associated with polypeptides at Rf values of 0.47 and 0.64–0.74 in the post-ethanol fraction compared with the crude extract (Figure 2B). When equal amounts of protein from the crude extract and the post-ethanol fraction were analyzed (Figure 2, lanes B1 and B3, respectively), both the rate and final intensity of color development in the CA activity zones were significantly greater in the post-ethanol fraction. A pronounced CA overload was observed when the post-ethanol fraction was analyzed at 20 µg (Figure 2, lane B3). Notably, even when half this amount was applied (lane B2), CA activity remained substantially higher than that observed in the crude extract (lane B1). Collectively, the data presented in Figure 2 and Table 1 demonstrate that the treatment of the leaf protein extract with 90% ethanol effectively removes RuBisCo while retaining most of the carbonic anhydrase activity in the post-ethanol fraction.

3.3. CA Activity sources indicated by Protonography

The protonography technique was used in accordance with the method described by De Luca et al. (2015) to study the sources of CA activity among soluble proteins in *C. album* leaves. Protonography allows the visualization of CA hydratase activity in a gel following electrophoresis in the presence of SDS, which disintegrates CA-containing complexes. SDS inhibits hydratase activity, which is subsequently restored during the incubation of the gel in a Triton X-100 solution. When the gel is then placed in CO_2-saturated water, CA activity manifests as a change in the color of the BTB indicator from blue to yellow.

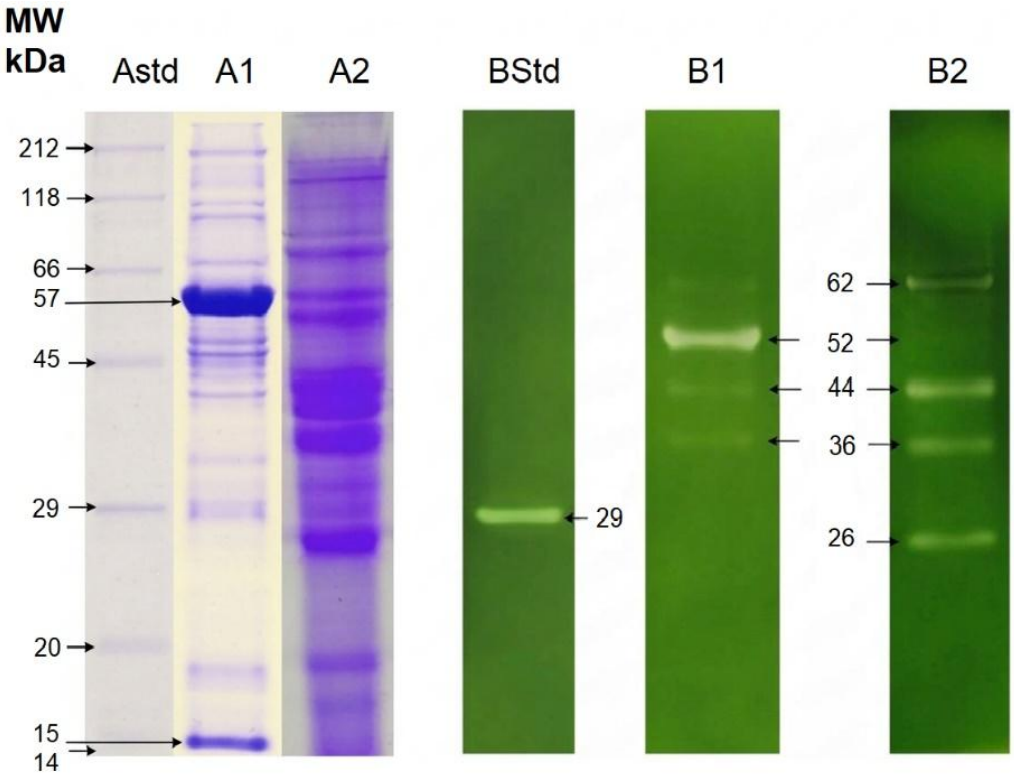


Figure 3. SDS-PAGE and protonography of soluble proteins isolated from *C. album* leaves. The polypeptides in the marker mixture (lane A Std), the crude extract (lane A1) and the post-ethanol fraction (lane A2) were stained with Coomassie brilliant blue. CA activity was visualized by protonography in the protein standarts (B Std), the crude extract (lane B1) and the post-ethanol fraction (lane B2), using the BTB indicator.
The CA activity in the protein standards (B Std) corresponds to human CA (29kDa) from the Protein Marker III (PanReacApplicam) mixture. Electrophoretic analyses were performed simultaneously under denaturing but non-reducing conditions, as described by De Luca et al. (2015). The apparent molecular weights (MW) of polypeptides on these gels were determined by plotting the logarithmic MW of standard protein markers against their relative migration distance (Rf). Full-length, uncropped original gels are presented in Supplementary File 1.

Figure 3 shows a comparison of SDS-PAGE gels indicating the distribution of polypeptides and protonography of CA activity in *C. album* leaf soluble proteins in the crude

extract and post-ethanol fraction. Analysis of the Coomassie-stained gel (Figure 3) revealed the two most intense polypeptide bands in the crude extract of C. album leaves, with estimated MWs of 57 and 15 kDa, respectively (lane A1). These are likely to correspond to the large (RbcL) and small (RbcS) subunits of RuBisCo, which is the main soluble chloroplast protein. This aligns with previous research indicating that RbcL subunits have MWs of approximately 51–58 kDa, while RbcS subunits range from 12 to 18 kDa (Jensen and Bahr 1977). The polypeptide profile of the post-ethanol fraction (Figure 3, lane A2) differed significantly from that of the crude extract. The 15-kDa polypeptide (presumably RbcS) was practically absent. Two polypeptides were detected in the 51–58 kDa range on the electropherogram, which apparently cannot be RbcL (Figure 3, lane A2). Thus, the results of both native electrophoresis (Figure 2) and SDS-PAGE (Figure 3) indicate that the enzyme RuBisCo is irreversibly denatured and becomes insoluble in an aqueous buffer after the treatment of *C. album* leaf protein extract with high concentrations of ethanol.

CA activity visualization using protonography also shows significant differences between proteins in the crude extract and post-ethanol fraction (Figure 3, lanes B1 and B2). Three carriers of CA activity were identified in the crude extract of *C. album* leaves, with apparent MWs of 36 kDa, 44 kDa, and 52 kDa detected using the Rf-log MW plot. In addition to these polypeptides, 25–26 kDa and 62 kDa polypeptides were identified in the post-ethanol extract. These polypeptides are likely part of multiprotein complexes that disintegrate due to ethanol treatment, releasing the CAs that comprise them.

3.4. Esterase Isoenzymes of C. album Leaves

CA in C_3 plants is known to be represented by the α-, β-, and γ-families (Fabre et al. 2007; DiMario et al. 2017; Momayyezi et al. 2020). Unlike β- and γ-types, α-CA can catalyze non-physiological reactions, including the hydrolysis of nitrophenol esters. The different structure of α-CA allows it to bind and react with a wider variety of substrates than the more specialized active sites of β- and γ-CA (Höst et al. 2006). The rate of the esterase reaction using artificial substrates is a common method for evaluating α-CA activity from human and animal tissues (Uda et al. 2015).

In this study, we attempted to identify the α-form of CA by simultaneously visualizing CA and esterase activities in the post-ethanol protein fraction of *C. album* leaves after SDS-PAGE under denaturing but non-reducing conditions (De Luca et al. 2015). The results presented in Figure 4 show the distribution of esterase and CA isoenzymes in the gel. A total of twelve esterase-active zones were resolved in the post-ethanol fraction of C. album leaves,

two of which are positively correlated with CA-active zones with apparent MWs of approximately 62 and 25–26 kDa. These CA-active zones were detected in the gels after the SDS treatment of the post-ethanol leaf fraction (Figure 3, lanes B1 and B2). It can be assumed that the 62 and 25–26 kDa polypeptides were part of the multiprotein complexes that were disrupted by the SDS treatment. It is evident that the classification of carbonic anhydrase (CA) as an α-type enzyme, based solely on esterase activity, is an indirect approach and can be considered only as a preliminary suggestion.

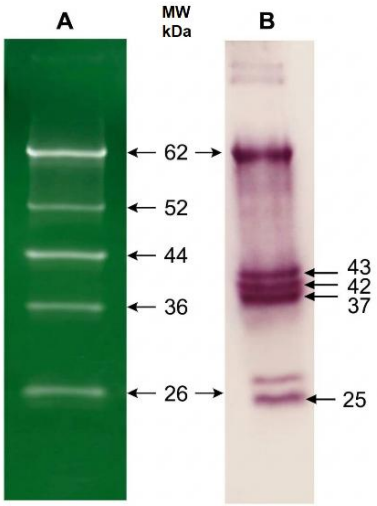


Figure 4. **Visualization of CA and esterase activities in the post-ethanol protein fraction from *C. album* leaves**. following SDS-PAGE was performed under denaturing, non-reducing conditions according to De Luca et al. (2015). CA (lane A) and esterase (lane B) activities were visualized sequentially in the same gel. CA activity was first detected for 5–10 min, after which the gel was photographed, thoroughly washed, and subsequently incubated with β-naphthyl acetate. Esterase activity was visualized as an insoluble violet azo dye formed in the presence of Fast Blue BB salt, as described by Kumar et al. (2019; 2022). Full-length, uncropped original gels are presented in Supplementary File 1.

3.5. The effects of heavy metal ions on CA activity in C. album leaf soluble proteins

Studies of CA activity in tissues and isolated enzymes of various animals, including humans, have demonstrated that HM are among the most effective natural CA inhibitors (Kaya et al. 2013; Kucuk and Gulcin 2016; Demirdağ et al. 2013; Lionetto et al. 2012; 2016: Caricato et al. 2019;). The vast majority of enzymes that have been examined in this particular context are classified as α-CA. In contrast, there is only fragmentary data on the effect of certain HM ions on β-CA, which is found mainly in bacteria, plants, and algae. Based on the available literature and our recent studies into the impact of HMs on total CA activity in soluble leaf proteins of New Zealand spinach, we concluded that plant CAs are more susceptible to inhibition by Ag^{+}, Hg^{2+}, Cd^{2+} and Cu^{2+} than α-CA (Zolotareva et al. 2025).

In this study, we measured the effects of the *in vitro* inhibition of CA activity in soluble leaf protein fraction of *C. album* by Ag^{+}, Hg^{2+}, Cd^{2+}, Cu^{2+}, Zn^{2+} and Pb^{2+}. The data presented in Figure 5, 8, 9 illustrate the correlation between the CA hydratase activity of the post-ethanol fraction of soluble proteins from *C. album* leaves and the concentration of HM ions. Enzyme activities were measured in the presence of different concentrations of HM salts. Control enzyme activity in the absence of a metal ion was taken as 100%. For each HM ion, an activity percentage versus inhibitor concentration tube was drawn.

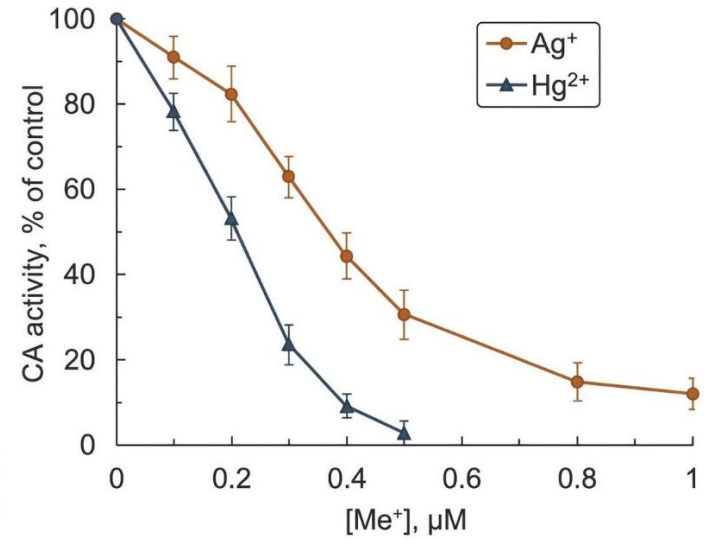


Figure 5. The effect of Ag^{+} and Hg^{2+} ions on CA activity of the post-ethanol fraction of soluble proteins isolated from *C. album* leaves. An assay was performed at 0°C after pre-incubating the enzyme-containing fraction with various metal concentrations at room temperature for five minutes. Bars represent the mean relative CA activity ± SD obtained from five independent experiments. Statistical significance was evaluated using Student's t-test; $P < 0.01$, degrees of freedom (df) = 13.

As shown in Figure 5, CA activity was inhibited by submicromolar concentrations of mercury and silver ions. Actual ratios of metal ions per 1 µg of protein ranged from 0,005 to 0,022 nmol/µg protein for Hg^{2+} and from 0.005 to 0.05 nmol/µg protein for Ag^{+}.

To assess the effect of silver ions on the activity of various CA isoforms, electrophoretic analysis of soluble protein fractions from *C. album* leaves pretreated with various concentrations of $AgNO_3$ was performed. The results are presented in Figure 6.

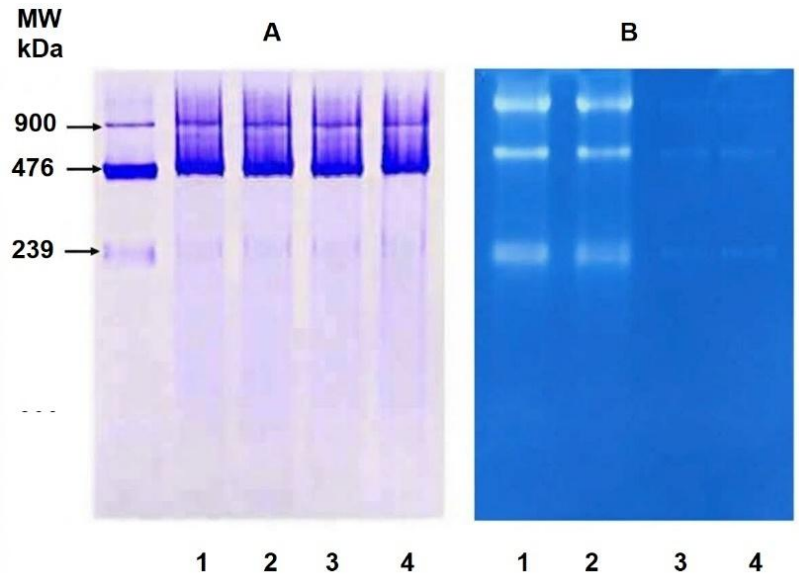


Figure 6. Visualization of proteins and CA activity in PAGE in crude extracts from *C. album* leaves pre-incubated with different concentrations of $AgNO_3$. Prior to gel loading, samples were incubated with $AgNO_3$ for 10 min. The $AgNO_3$-to-protein ratios were 0.01 (lane 2), 0.02 (lane 3), and 0.04 (lane 4) nmol $AgNO_3$ per μg protein. Lane 1 represents the control. Panel A: Coomassie Brilliant Blue–stained soluble proteins. Protein markers include horse spleen ferritin dimer (900 kDa), horse spleen ferritin monomer (476 kDa), and catalase (239 kDa). Panel B: In-gel visualization of CA activity after native electrophoresis. Full-length, uncropped original gels are presented in Supplementary File 1.

As can be seen, the intensity of staining of all protein zones exhibiting CA activity in the gel was reduced in $AgNO_3$-pretreated samples. Inhibition of enzymatic activity was not eliminated during protein electrophoresis, indicating irreversible silver binding. The effective Ag^+/protein ratio corresponded to the ratio in the solution (see Figure 5). The mobility of protein bands that migrated at rates similar to markers 239 and 476 kDa in preparations pretreated with $AgNO_3$ was slightly reduced (see Figure 6). This may be due to a decrease in the surface charge of the proteins caused by Ag^+ binding to negatively charged surface groups.

A similar effect was observed when the protein fraction extracted from the *C. album* leaves was incubated with various concentrations of $CdCl_2$ (Figure 7). It can be seen that the level of staining of protein zones with CA activity decreases in samples pre-incubated with $CdCl_2$.

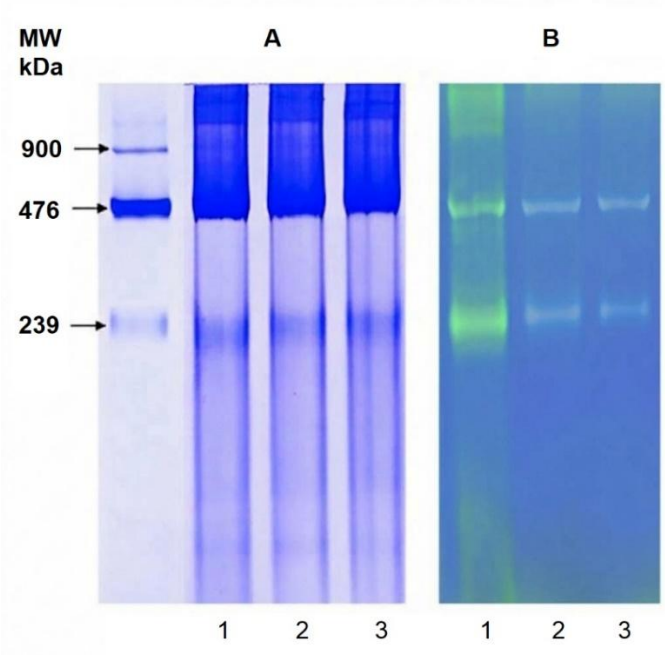


Figure 7. Visualization of proteins and CA activity in PAGE in crude extracts from *C. album* leaves pre-incubated with different concentrations of $CdCl_2$. Prior to gel loading, samples were incubated with $CdCl_2$ for 10 min. The $CdCl_2$-to-protein ratios were 0.1 (lane 2) and 0.15 (lane 3) nmol $CdCl_2$ per µg protein. Lane 1 represents the control.
Panel A: Coomassie Brilliant Blue–stained soluble proteins. Protein markers are the same as those described in the legend for Figure 6.
Panel B: In-gel visualization of CA activity after native electrophoresis.
Full-length, uncropped original gels are presented in Supplementary File 1.

Figure 8 shows a comparison of the dose–response curves of CA activity in soluble *C. album* proteins in the presence of Cu^{2+} and Cd^{2+} ions. Suppression of enzymatic activity was observed in the concentration range of 5–100 µM, with slightly higher concentrations of Cu^{2+} required to achieve inhibition levels comparable to those induced by Cd^{2+}.

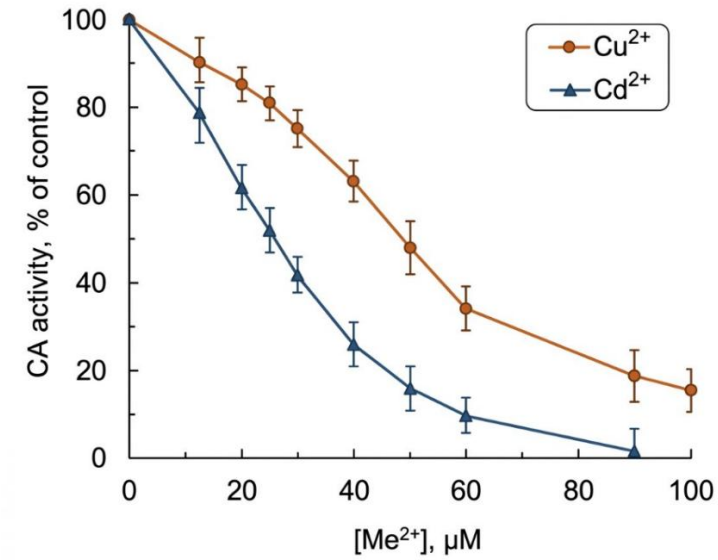


Figure 8. The effect of different concentration of Cu^{2+} and Cd^{2+} ions on CA activity of the post-ethanol fraction of soluble proteins isolated from *C. album* leaves. The measurement conditions are the same as those in the caption to Figure 5.

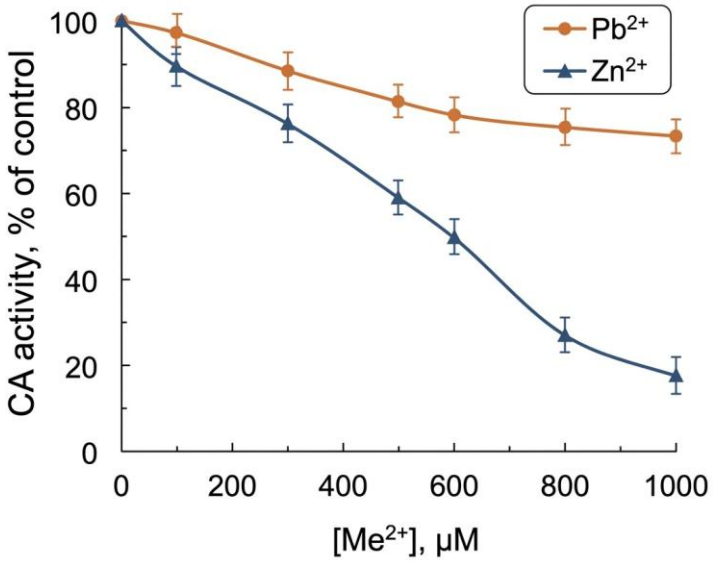


Figure 9. The effect of Zn^{2+} and Pb^{2+} ions on the CA activity of the post-ethanol fraction of soluble proteins isolated from *C. album* leaves. The measurement conditions are the same as those in the caption to Figure 5.

Figure 9 illustrates the dependence of carbonic anhydrase (CA) activity on the concentrations of Zn^{2+} and Pb^{2+} ions in soluble *C. album* proteins. Inhibition of enzymatic activity was observed over the concentration range of approximately 2–1000 μM, with Pb^{2+} exhibiting a markedly weaker inhibitory effect on CA activity than Zn^{2+}. Notably, Pb^{2+} at a concentration of 1 mM reduced CA activity by only 20%.

Overall, the extent of CA inhibition varied substantially depending on the type of heavy metal (HM) present, as demonstrated by the results shown in Figure 5–7. In addition, the effect of a specific CA inhibitor, acetazolamide (AZ), was investigated.

To quantitatively compare the inhibitory potency of different effectors, the half-maximal inhibitory concentration (IC_{50})—defined as the concentration required to reduce enzyme activity by 50%—was determined. Table 2 summarizes the estimated IC_{50} values derived from the CA activity–inhibitor concentration curves.

Table 2

Inhibition of hydratase activity in the total fraction of soluble proteins isolated from *C. album* leaves by heavy metal ions and acetazolamide

HM ions	Hg^{2+}	Ag^{+}	Cd^{2+}	Cu^{2+}	Zn^{2+}	Acetazolamide
IC_{50}*, μM	0.28±0.02	0.35±0.04	20±3	50±5	550±70	18±2

IC_{50} values were determined by nonlinear regression of inhibition curves using a four-parameter logistic model. Errors of IC_{50} were expressed as 95% confidence intervals calculated from the fitted model.

According to our data, the IC_{50} for the inhibition of CA activity by AZ in the leaf protein fraction is estimated to be 16–20 μM (Table 2). These levels are consistent with those typically observed for plant CAs and differ from those observed for animal α-CAs, which is much more sensitive to sulfonamide inhibition (Pocker, 1990; Johansson and Forsman 1993; Rowlett, 2010; Dinçer et al. 2016). Additionally, unlike Ag^{+} (Figure 6) and Cd^{2+} (Figure 7), CA activity in gels was not suppressed after the electrophoretic separation of the *C. album* leaf protein fraction that was preincubated with various AZ concentrations. This suggests that the enzyme is released from the inhibitor during electrophoretic separation, indicating that acetazolamide inhibition is reversible.

4. Discussion

CA accounts for up to 2% of the total protein in the leaves of C_3 plants (Okabe et al. 1984; Peltier et al. 2006), making it the second most abundant cellular protein after RuBisCo. Higher plants possess three distinct CA families (α, β, γ), each represented by multiple isoforms due to alternative splicing (DiMario et al. 2017; Shen et al. 2021; Tognacca et al. 2023), which is crucial for environmental adaptation (Eckardt 2013). In C_3 plant leaves, the highest concentration of CA, specifically β-CA1, is found in the stroma of chloroplasts, with smaller amounts present in the cytosol.

The stroma is the semi-fluid interior of the chloroplast that contains the water-soluble enzymes of the Calvin cycle. The most abundant of these enzymes is RuBisCo, which

accounts for 30–65% of the total protein content in plant leaves (Grácio et al. 2023). Due to its high concentration, this large multi-subunit enzyme complex (~550 kDa) often overloads electrophoretic and chromatographic systems. This makes it difficult to isolate and detect minor leaf proteins during analytical procedures; thus, specialized purification methods are required to analyze less abundant proteins.

This study revealed that the soluble protein profile was drastically reshaped after the two-stage fractionation of the crude *C. album* leaf extract, highlighting important differences in protein stability. The total amount of water-soluble proteins decreased by almost 29-fold following ethanol precipitation (Table 1), suggesting that high ethanol concentrations irreversibly denature most leaf proteins, including RuBisCo. In contrast, a substantial portion of CA activity was recoverable. Although the total CA activity decreased 2.5-fold, the specific activity increased approximately 11-fold, rising from about 186 WAU·(mg protein)$^{-1}$ in the crude extract to ~2100 WAU·(mg protein)$^{-1}$ in the post-ethanol fraction (Table 1).

While this enrichment initially suggests that *C. album* CAs are highly resistant to ethanol-induced denaturation and can refold into an active conformation upon solvent removal—unlike the large, complex multi-subunit RuBisCo —the 2.5-fold loss in total CA activity indicates a more complex dynamic. This loss may result not only from partial irreversible denaturation but also from incomplete precipitation during the initial extraction stage. For instance, when proteins are precipitated from a 30% alcohol–water extract, a fraction of the CAs may remain in solution due to insufficient settling time or suboptimal precipitation parameters (e.g., temperature, pH, and salt concentration). Consequently, this partial loss of CA inherently favors the recovery and downstream selection of more ethanol-resistant CA isoforms in the final fraction. As this is the first study to characterize CA isoforms in *C. album*, the precise structural rationales dictating these differing responses to ethanol remain to be fully elucidated. Future targeted studies utilizing model plants, such as *Arabidopsis thaliana* or *Pisum sativum*, will be required to determine the exact mechanistic causes of this differential solubility and to optimize the conditions for the complete re-precipitation of CA. Ultimately, this fractionation strategy successfully yielded a protein fraction nearly free of RuBisCo, with a specific CA activity more than ten times higher than the initial level.

Non-denaturing electrophoretic analysis revealed three zones of CA activity after visualization in both the post-ethanol fraction and the crude leaf extract: the most intense zone (Rf ~0.47), a wide band (Rf ~0.64–0.74), and a weak zone in the region of high-molecular-weight (MW) proteins (Rf ~0.32) (Figure 2). The zones in the post-ethanol fraction were significantly more intense than those in the original extract. The electrophoretic mobility of the protein exhibiting the highest CA activity (Rf ~0.47) closely matches that of a protein

marker with a molecular weight of 239 kDa (A1–A3, Figure 2). This value aligns with the estimated molecular mass of leaf β-carbonic anhydrases in various C_3 plant species, which ranges from 180 to 250 kDa and corresponds to octamers composed of eight identical subunits with monomer masses varying from 26 to 34 kDa (Graham et al. 1984; Kandel et al. 1978; Rumeau et al. 1996; Björkbacka et al. 1997). In this study, in addition to the zone at Rf ~0.47, a broad band of CA activity (Rf ~0.64–0.74) was also detected. According to the literature, at least two forms of CA have been identified in the soluble protein fraction of various higher plant species using electrophoretic or isoelectric focusing analyses (Atkins et al. 1972; Kachru and Anderson 1974; Graham et al. 1984). These isoforms are thought to occupy distinct cytoplasmic and chloroplast locations. The vast majority of CA activity in C_3 plants is localized in the chloroplast stroma (DiMario et al. 2017). At the same time, cytoplasmic CA activity in potato leaves accounts for about 13% of the total (Rumeau et al.1996). Both the extrachloroplastic and chloroplastic β-family enzymes are octamers with high molecular masses of 255 kDa and 220 kDa, respectively (Rumeau et al. 1996). The spinach chloroplastic enzyme consists of 26-kDa monomers (Kandel et al. 1978), whereas the potato chloroplastic enzyme comprises two distinct subunits: a dominant subunit of 27 kDa and a minor subunit of 27.5 kDa. The monomer of the potato extrachloroplastic CA is estimated to be a 30-kDa polypeptide (Rumeau et al. 1996).

Studies of the isolated cDNAs that encode the chloroplast CAs of spinach and pea (Burnell et al. 1990; Fawcett et al. 1990; Majeau and Coleman 1991) revealed that CAs are generally synthesized as larger precursors (approximately 34–35 kDa) in the cytoplasm. Then, they are transported into the chloroplast, where they are processed into mature proteins weighing 25.5 kDa in spinach (Fawcett et al. 1990) and 24.2 kDa in pea (Majeau and Coleman 1991).

The protonography method was used to identify three enzymatically active polypeptides in the crude leaf extract and five isoforms in the fraction obtained after ethanol treatment. Isoforms with molecular weights of 52, 44, and 36 kDa were present in both fractions (Figure 3, B1 and B2). Additionally, 62-kDa and 26-kDa isoforms were present only in the post-ethanol fraction. The 52-kDa polypeptide is significantly more intensely stained in the crude extract than in the post-ethanol fraction. Conversely, a 26-kDa band appears after treatment with ethanol. This redistribution of CA activity may be associated with the breakdown of some of the 52-kDa polypeptides during ethanol treatment. Since SDS solubilization during protonography is performed under non-reducing conditions that exclude boiling, the complete disruption of the polypeptide complexes may not occur. Consequently, the appearance of

586 additional polypeptides during the analysis of the post-ethanol fraction may result from the
587 denaturing effect of the high ethanol concentrations used in the preliminary preparation.
588 In this study, native electrophoresis detected three polypeptide complexes with CA
589 activity (Figure 3), whereas visualization of the enzymatic activity following protonography
590 revealed five polypeptides. The oligomeric forms of plant carbonic anhydrases (CAs) generally
591 consist of identical β-type monomers (Rowlett, 2010). β-CAs are the predominant class of CAs
592 in plants and are typically represented by a moderate-sized gene family containing four to seven
593 genes in most plant species (Fabre et al. 2007; DiMario et al. 2017; Momayyezi et al. 2020).
594 Genetic studies with GFP fusions and mutant analysis in Arabidopsis have confirmed that β-
595 CA1 and β-CA5 are located specifically within the chloroplast stroma in leaf mesophyll cells.
596 β-CA5 is expressed throughout the plant, including in the roots, but its expression is less
597 common than β-CA1 in leaves. Alternative splicing of the β-CA1 gene produces at least four
598 distinct, functional mRNA transcripts. These transcripts are translated into four protein
599 isoforms: β-CA1.1, β-CA1.2, β-CA1.3, and β-CA1.4 (Shen et al. 2021). β-CA1.1 and β-CA1.2
600 show strong signals in the chloroplast stroma, while β-CA1.3 accumulates in the chloroplast
601 envelope. β-CA1.4 is often associated with the cytoplasm. Functional genetics reveals that β-
602 CA2 and β-CA3 isoforms are primarily located in the cytoplasm/cytosol (DiMario et al. 2016).
603 Thus, the results of this study suggest that multiple and spliced forms of β-CA can be at least
604 partially detected by protonography.
605 In this study, the in situ visualization of esterase activity was used for the preliminary
606 identification of two isoforms of α-carbonic anhydrase (α-CA) in the soluble protein fraction
607 of leaf tissue (Figure 4). The esterase activity of CA reflects its ability to hydrolyze activated
608 esters and represents a “nonspecific” secondary function in addition to its primary catalytic
609 reaction—CO_2 hydration. This activity is characteristic of α-class carbonic anhydrases, which
610 use the same active site for both esterase reactions and CO_2 hydration (Uda et al. 2015). In
611 contrast, no detectable esterase activity has been reported for enzymes of the β- and γ-CA
612 families (DiMario et al. 2016).
613 Thus, simultaneously detecting CA and esterase activity allows us to tentatively identify
614 protein bands with MWs of 25–26 and 62 kDa (Figure 4) as α-CA. Higher plants generally
615 possess multiple α-CA gene copies, with isoforms found in various tissues and cellular
616 compartments (Langella et al. 2022). Clear information on the intracellular location of these α-
617 CA isoforms is available only for α-CA1, which is located in the chloroplast stroma (Villarejo
618 et al. 2005; DiMario et al. 2017). These α-CAs can form homodimers, stabilized by hydrogen
619 bonds and hydrophobic interactions (Buren et al. 2011).

Although α- and β-CAs share common catalytic features, such as CO_2 hydration activity and the use of zinc ions as metal cofactors, significant structural differences exist between them. First, most α-CAs form monomers or dimers, whereas β-CAs occur in various oligomeric states, including dimers, tetramers, hexamers, and octamers (Kimber and Pai, 2000). Second, α-CA structures are strongly coordinated by three histidine residues and a water molecule in the active site (Liljas et al. 1972; Eriksson et al. 1988), whereas β-CAs utilize two cysteine residues and one histidine residue. This makes the β-CA active site more negatively charged and structurally distinct (Kimber and Pai, 2000). Despite these differences, both classes effectively catalyze the rapid conversion of CO_2 to bicarbonate and protons with similar catalytic efficiencies. At the same time, these CA classes differ greatly in their sensitivity to inhibitors. For example, α-CAs, commonly found in animals, are strongly inhibited by nanomolar concentrations of sulfonamides, such as acetazolamide (AZ) (https://www.aatbio.com/data-sets/carbonic-anhydrase-inhibitors-ic50-ki; Supuran et al. 2003). In contrast, enzymes from higher terrestrial plants are much less sensitive to inhibition by sulfonamides: half-maximal inhibition (IC_{50}) is observed at AZ concentrations ranging from 20 to 500 μM (Pocker and Ng 1973; Johansson and Forsman 1993; Graham et al. 1984; Sültemeyer et al. 1993). In this study, the IC_{50} of CA activity in the protein fraction of *C. album* leaves occurred with the addition of 16–20 μM acetazolamide, a concentration 100–1000 times higher than that typically required to inhibit animal CAs.

Many studies have shown that metal ions, such as Cd^{2+}, Cu^{2+}, Zn^{2+}, and Pb^{2+}, inhibit α-CA activity in human and animal tissues, fish erythrocytes, and crustacean brains and gills. These ions have specific Ki or IC_{50} values ranging from the micromolar to the millimolar level (Ekinci et al. 2007; Lionetto et al.2012, 2016). However, only a few studies have addressed the effects of metal ions on plant CAs, which are mainly represented by β-isoforms (Asencio and Cedeño-Maldonado 1979; Polishchuk et al. 2018; Topchiy et al. 2019; Zolotareva et al. 2025). Available data suggest that plant CAs are more sensitive to inhibition by certain heavy metals (HMs) (such as Hg^{2+}, Ag^{+}, Cd^{2+}, and Cu^{2+}) than animal CAs, partly due to the high affinity of the cysteine residues in the β-CA active site for HMs.

Studies on the impact of increasing HM concentrations on the CA activity of the protein fraction from *C. album* leaves revealed that, although HMs typically function as inhibitors, the intensity of their inhibitory impact varies (Figure 5–9).

Hg^{2+} ions were the strongest inhibitors, suppressing 50% of the initial enzyme activity at concentrations of 0.20–0.24 μM (Figure 5). The IC_{50} for Ag^{+} was 0.36–0.40 μM (Figure 5). Cd^{2+} and Cu^{2+} ions inhibited the hydratase activity of the soluble protein fraction from *C. album* leaves at concentrations nearly 100 and 200 times higher than the IC_{50} values for Hg^{2+},

respectively (Figure 8). Zn^{2+} and Pb^{2+} were found to be significantly weaker inhibitors. As shown in Figure 9, 1 mM of Zn^{2+} inhibited the CA activity of the leaf protein fraction by approximately 80%, whereas 1 mM of Pb^{2+} inhibited it by only about 20%. Although Zn^{2+} ions are essential cofactors for the catalytic activity of CAs, high concentrations of exogenous Zn^{2+} generally inhibit CA activity by binding to histidine/cysteine residues and disrupting the proton transfer mechanism in the active site, or by binding to regions undergoing conformational changes. While higher concentrations act as inhibitors, low concentrations of Zn^{2+} may enhance or have negligible effects on activity (Lionetto et al. 2016). Comparing the conditions under which Zn^{2+} ions inhibit CA in *C. album* leaves with literature data on the effects of exogenous Zn^{2+} on α-CA activity in various organisms (Lionetto et al. 2012, 2016) reveals that both classes of CAs are inhibited within a similar concentration range (IC_{50} approximately 0.4–0.6 mM). This suggests that the mechanisms by which Zn^{2+} ions inhibit carbonic anhydrase in plants and animals may be conserved.

As demonstrated in the present study and in previous research (Zolotareva et al. 2025), lead ions are weak inhibitors of plant CAs. However, it should be noted that animal α-CAs are more sensitive to Pb^{2+} inhibition (Tu et al. 2012; Ceyhun et al. 2011; Calhoun et al. 1985). Pb^{2+} can replace the native Zn^{2+} in α-CAs; the resulting enzyme has significantly reduced activity compared to the native Zn-CA due to structural differences and the lower efficiency of Pb^{2+} in the catalytic mechanism. Pb^{2+} ions bind within the α-CA active site cavity and often interact with tyrosine residues rather than native histidine residues, resulting in an inactive, structurally altered α-CA enzyme (Tu et al. 2012; Calhoun et al. 1985). Due to these structural differences, it can be hypothesized that the accessibility of the active site of plant CAs to Pb^{2+} ions is more limited than that of animal CAs. Consequently, we propose that the determined IC_{50} values and inhibition profiles can be used as guidelines for estimating the range of subinhibitory concentrations for HM ions, which we define as concentrations that cause the inhibition of total CA activity at a level of ≤20–25%.

5. Conclusion

Carbonic anhydrase (CA) is widely regarded as a sensitive indicator of physiological stress in plants because its activity responds rapidly to environmental perturbations, including HM pollution. However, the responses of plant CAs to metal stress remain insufficiently characterized and have been investigated in only a limited number of species.

Chenopodium album (L.) is a widely distributed, fast-growing weed that thrives across diverse geographical and ecological conditions, including heavily contaminated habitats. In this study, *C. album* was evaluated as a potential plant bioindicator for assessing HM

contamination in terrestrial environments. Biochemical analysis of a soluble protein fraction depleted of RuBisCo and enriched in CA, combined with protonography, revealed the presence of at least five distinct CA-related activity bands, providing new insight into the diversity of CA isoforms in this species. CA activity exhibited pronounced and differential responses to HM exposure, supporting its potential utility as an early biochemical marker of environmental stress.

Among the metals examined, Hg^{2+} and Ag^{+} caused strong inhibition of CA activity at submicromolar concentrations, whereas Cd^{2+} and Cu^{2+} produced moderate inhibitory effects, and Zn^{2+} and Pb^{2+} showed weak or negligible inhibition. Although the present study establishes the in vitro sensitivity of CA to a range of heavy metals, extrapolation of these findings to environmental biomonitoring requires careful consideration of environmentally relevant exposure conditions. The IC_{50} values determined in this study—ranging from submicromolar concentrations for Hg^{2+} and Ag^{+} to 20–50 μM for Cd^{2+} and Cu^{2+}—fall within concentration ranges that may occur in contaminated environments. Plants growing in metal-polluted soils actively uptake and bioaccumulate these elements in their aerial tissues, potentially allowing intracellular metal concentrations to approach levels that inhibit CA activity.

Nevertheless, because metal bioavailability, transport, and compartmentalization are strongly influenced by physiological and environmental factors in intact plants, further *in vivo* studies are required to fully validate the suitability of specific CA isoforms as robust biomarkers of HM pollution. The high sensitivity of CA to Hg^{2+} and Ag^{+} is likely associated with the presence of cysteine residues in the active sites of plant β-type CAs, rendering these enzymes particularly vulnerable to metals with strong affinity for sulfhydryl groups. Notably, CAs from *C. album* appear to be more sensitive to several toxic metals than their animal counterparts, which may enhance their diagnostic value for environmental monitoring.

Abbreviations

BTB – bromothymol blue;

CA – carbonic anhydrase;

HM – heavy metals;

RuBisCo - ribulose-1,5-bisphosphate carboxylase/oxygenase

WAU – Wilbur-Anderson Units

Ethics approval and consent to participate

All methods involving plant and extracts were carried out in accordance with relevant institutional, national, and international guidelines and legislation. No human participants or animals were involved in this study

Consent for publication

All authors have reviewed and approved the final version of this manuscript for publication.

Availability of data and materials

The datasets generated and/or analyzed during the current study are available from the corresponding author on reasonable request. Uncropped original electrophoretic gel images are provided in Supplementary File 1.

Competing Interests

The authors declare no competing interests.

Funding

This work was supported by the National Academy of Science of Ukraine (Project# 0121U114515).

Authors' contributions

E.K.Z.: conceptualization, methodology, formal analysis, writing (original draft, review, and editing). N.M.T.: investigation, methodology, formal analysis, data curation and writing – review & editing. O.B.O.: investigation, formal analysis and data curation. All authors have read and agreed to the published version of the manuscript.

Acknowledgments The authors would like to express their deep gratitude to Professor Sergiy L. Mosyakin, a leading specialist in plant systematics and the taxonomy of Chenopodium at the M. G. Kholodny Institute of Botany in Kyiv, for formal taxonomic identification of the plant material as *Chenopodium album* sensu stricto. The authors are especially grateful to a leading engineer Viktoria Dadyka for technical support and plant care.

References

Aloud SS, Alotaibi KD, Almutairi KF, Albarakah FN (2023) Phytoremediation potential of native plants growing in industrially polluted soils of Al-Qassim, Saudi Arabia. Sustainability 15:2668. https://doi.org/10.3390/su15032668

Anderson LE, Carol AA (2004) Enzyme co-localization with Rubisco in pea leaf chloroplasts. Photosynth Res 82:49–58. https://doi.org/10.1023/B:PRES.0000040443.92346.37

Asencio CI, Cedeno-Maldonado A (1978) Effects of cadmium on carbonic anhydrase and activities dependent on electron transport of isolated chloroplasts. J Agric Univ Puerto Rico 63:195–201. https://doi.org/10.46429/jaupr.v63i2.10276

Atkins CA, Patterson BD, Graham D (1972) Plant carbonic anhydrases: I. Distribution of types among species. Plant Physiol 50:214–217. https://doi.org/10.1104/pp.50.2.214

Björkbacka H, Johansson IM, Skärfstad E, Forsman C (1997) The sulfhydryl groups of Cys 269 and Cys 272 are critical for the oligomeric state of chloroplast carbonic anhydrase from *Pisum sativum*. Biochemistry 36:4287–4294. https://doi.org/10.1021/bi962825k

Bradford MM (1976) A rapid and sensitive method for the quantitation of microgram quantities of protein utilizing the principle of protein-dye binding. Anal Biochem 72:248–254. https://doi.org/10.1016/0003-2697(76)90527-3

Buren S, Ortega-Villasante C, Blanco-Rivero A, Martinez-Bernardini A, Shutova T, Shevela D, Bako L, Villarejo A, Samuelsson G (2011) Importance of post-translational modifications for functionality of a chloroplast-localized carbonic anhydrase (CAH1) in *Arabidopsis thaliana*. PLoS One 6:e21021. https://doi.org/10.1371/journal.pone.0021021

Calhoun LA, Livesey DL, Mailer K, Addetia R (1985) Interaction of lead ions with bovine carbonic anhydrase: further studies. J Inorg Biochem 25:261–275.

Capasso C, De Luca V, Carginale V, Cannio R, Rossi M (2012) Biochemical properties of a novel and highly thermostable bacterial α-carbonic anhydrase from *Sulfurihydrogenibium yellowstonense* YO3AOP1. J Enzyme Inhib Med Chem 27:892–897. https://doi.org/10.3109/14756366.2012.703185

Caricato R, Giordano ME, Schettino T, Maisano M, Mauceri A, Giannetto A et al (2019) Carbonic anhydrase integrated into a multimarker approach for the detection of the stress status induced by pollution exposure in *Mytilus galloprovincialis*: a field case study. Sci Total Environ 690:140–150. https://doi.org/10.1016/j.scitotenv.2019.06.446

Ceyhun SB, Şentürk M, Yerlikaya E, Erdoğan O, Küfrevioğlu Öİ, Ekinci D (2011) Purification and characterization of carbonic anhydrase from the teleost fish *Dicentrarchus labrax* liver and toxicological effects of metals on enzyme activity. Environ Toxicol Pharmacol 32:69–74. https://doi.org/10.1016/j.etap.2011.03.013

Chibuike GU, Obiora SC (2014) Heavy metal polluted soils: effect on plants and bioremediation methods. Appl Environ Soil Sci 2014:752708. https://doi.org/10.1155/2014/752708

De Luca V, Del Prete S, Supuran CT, Capasso C (2015) Protonography, a new technique for the analysis of carbonic anhydrase activity. J Enzyme Inhib Med Chem 30:277–282. https://doi.org/10.3109/14756366.2014.917085

Del Prete S, Vullo D, De Luca V, Carginale V, Osman SM, AlOthman Z et al (2016) Comparison of the sulfonamide inhibition profiles of the α-, β- and γ-carbonic anhydrases from the pathogenic bacterium *Vibrio cholerae*. Bioorg Med Chem Lett 26:1941–1946. https://doi.org/10.1016/j.bmcl.2016.03.014

Demirdağ R, Yerlikaya E, Şentürk M, Küfrevioğlu Öİ, Supuran CT (2013) Heavy metal ion inhibition studies of human, sheep and fish α-carbonic anhydrases. J Enzyme Inhib Med Chem 28:278–282. https://doi.org/10.3109/14756366.2011.640633

DiMario RJ, Quebedeaux JC, Longstreth DJ, Dassanayake M, Hartman MM, Moroney JV (2016) The cytoplasmic carbonic anhydrases βCA2 and βCA4 are required for optimal plant growth at low CO_2. Plant Physiol 171:280–293. https://doi.org/10.1104/pp.15.01990

DiMario RJ, Clayton H, Mukherjee A, Ludwig M, Moroney JV (2017) Plant carbonic anhydrases: structures, locations, evolution, and physiological roles. Mol Plant 10:30–46. https://doi.org/10.1016/j.molp.2016.09.001

Dinçer B, Ekinci AP, Akyüz G, Kurtoğlu İZ (2016) Characterization and inhibition studies of carbonic anhydrase from gill of Russian sturgeon fish (*Acipenser gueldenstaedtii*). J Enzyme Inhib Med Chem 31:1662–1665. https://doi.org/10.3109/14756366.2015.1076810

Eckardt NA (2013) The Plant Cell reviews alternative splicing. Plant Cell 25:3639. https://doi.org/10.1105/tpc.113.251013

Edwards LJ, Patton RL (1966) Visualization of carbonic anhydrase activity in polyacrylamide gel. Stain Technol 41:333–334. https://doi.org/10.3109/10520296609116335

Eriksson AE, Jones TA, Liljas A (1988) Refined structure of human carbonic anhydrase II at 2.0 Å resolution. Proteins 4:274–282. https://doi.org/10.1002/prot.340040406

Fabre N, Reiter IM, Becuwe-Linka N, Genty B, Rumeau D (2007) Characterization and expression analysis of genes encoding α and β carbonic anhydrases in *Arabidopsis*. Plant Cell Environ 30:617–629. https://doi.org/10.1111/j.1365-3040.2007.01651.x

Flores-Calla SS, Villanueva-Salas JA, Diaz-Rodriguez K, Gonzales-Condori EG (2024) Removal of lead, cadmium, and mercury in monometallic and trimetallic aqueous systems using *Chenopodium album* L. Scientifica 2024:6842159. https://doi.org/10.1155/sci5/6842159

González-González RB, Flores-Contreras EA, Gonzalez-Gonzalez E, Torres Castillo NE, Parra-Saldivar R, Iqbal HM (2022) Biosensor constructs for the monitoring of persistent emerging pollutants in environmental matrices. Ind Eng Chem Res 62:4503–4520. https://doi.org/10.1021/acs.iecr.2c00421

Gontero B, Lebreton S, Graciet E (2018) Multienzyme complexes involved in the Benson–Calvin cycle and in fatty acid metabolism. Annu Plant Rev Online, pp 125–157. https://doi.org/10.1002/9781119312994.apr0060

Grácio M, Oliveira S, Lima A, Ferreira RB (2023) RuBisCO as a protein source for potential food applications: a review. Food Chem 419:135993. https://doi.org/10.1016/j.foodchem.2023.135993

Graham D, Reed ML, Patterson BD, Hockley DG, Dwyer MR (1984) Chemical properties, distribution, and physiology of plant and algal carbonic anhydrases. Ann N Y Acad Sci 429:222–237. https://doi.org/10.1111/j.1749-6632.1984.tb12340.x

Gupta AK, Sinha S (2007) Phytoextraction capacity of *Chenopodium album* L. grown on soil amended with tannery sludge. Bioresour Technol 98:442–446. https://doi.org/10.1016/j.biortech.2006.01.015

Habibi F, Mosyakin SL, Shynder OI, Krak K, Čortan D, Filippi GA, et al. (2023) *Chenopodium ucrainicum* (Amaranthaceae), a new 'BB' genome diploid species: karyological, cytological, and molecular evidence. Bot J Linn Soc 203:401–410. https://doi.org/10.1093/botlinnean/boad032

Hines KM, Chaudhari V, Edgeworth KN, Owens TG, Hanson MR (2021) Absence of carbonic anhydrase in chloroplasts affects C3 plant development but not photosynthesis. Proceedings of the National Academy of Sciences, 118(33): e2107425118 https://doi.org/10.1073/pnas.2107425118

Hoang CV, Chapman KD (2002). Biochemical and molecular inhibition of plastidial carbonic anhydrase reduces the incorporation of acetate into lipids in cotton embryos and tobacco cell suspensions and leaves. Plant Physiol 128(4):1417-1427. https://doi.org/10.1104/pp.010879

Höst G, Mårtensson LG, Jonsson BH (2006) Redesign of human carbonic anhydrase II for increased esterase activity and specificity towards esters with long acyl chains. BBA Proteins Proteom 1764:1601–1606. https://doi.org/10.1016/j.bbapap.2006.07.010

Hu H, Rappel WJ, Occhipinti R, Ries A, Böhmer M, You L, Xiao C, Engineer CB, Boron WF, Schroeder JI (2015) Distinct cellular locations of carbonic anhydrases mediate CO_2 control of stomatal, movements. Plant Physiol 169:1168–1178. https://doi.org/10.1104/pp.15.00646

Igamberdiev AU (2015) Control of Rubisco function via homeostatic equilibration of CO_2 supply. Front plant sci 6:106. https://doi.org/10.3389/fpls.2015.00106

Index Herbariorum: a global directory of public herbaria and associated staff. New York Botanical Garden. 2026. https://sweetgum.nybg.org/science/ih/. Accessed 19 Nov 2026.

Jebanathirajah JA, Coleman JR (1998) Association of carbonic anhydrase with a Calvin cycle enzyme complex in *Nicotiana tabacum*. Planta 204:177–182. https://doi.org/10.1007/s004250050244

Jensen RG, Bahr JT (1977) Ribulose 1,5-bisphosphate carboxylase-oxygenase. Annu Rev Plant Physiol 28:379–400. https://doi.org/10.1146/annurev.pp.28.060177.002115

Johansson IM, Forsman C (1993) Kinetic studies of pea carbonic anhydrase. Eur J Biochem 218:439–446. https://doi.org/10.1111/j.1432-1033.1993.tb18394.x

Kachru RB, Anderson LE (1974) Chloroplast and cytoplasmic enzymes. Planta 118:235–240. https://doi.org/10.1007/BF00384779

Kandel M, Gornall AG, Cybulski DL, Kandel SI (1978) Carbonic anhydrase from spinach leaves. Isolation and some chemical properties. J Bio1 Chem 253: 679-685. https://doi.org/10.1016/S0021-9258(17)38156-5

Kaya ED, Söyüt H, Beydemir Ş (2013) Carbonic anhydrase activity from the gilthead sea bream (*Sparus aurata*) liver: the toxicological effects of heavy metals. Environ Toxicol Pharmacol 36:514–521. https://doi.org/10.1016/j.etap.2013.05.019

Kimber MS, Pai EF (2000) The active site architecture of *Pisum sativum* β-carbonic anhydrase is a mirror image of that of α-carbonic anhydrases. EMBO J 19:1407–1418. https://doi.org/10.1093/emboj/19.7.1407

Kucuk M, Gulcin I (2016) Purification and characterization of the carbonic anhydrase enzyme from Black Sea trout (*Salmo trutta labrax coruhensis*) kidney and inhibition effects of some metal ions on enzyme activity. Environ Toxicol Pharmacol 44:134–139. https://doi.org/10.1016/j.etap.2016.04.011

Kumar D, Behal S, Bhattacharyya R, Banerjee D (2022) Fast Blue B produces a light background on the gel surface. Indian J Clin Biochem 37:124–125. https://doi.org/10.1007/s12291-020-00913-6

Kumar D, Behal S, Bhattacharyya R, Banerjee D (2019) β-Naphthyl acetate in acetone produces a dark background for staining of esterase activity on gel. Indian J Clin Biochem 34:240–242. https://doi.org/10.1007/s12291-018-0769-3

Langella E, Di Fiore A, Alterio V, Monti SM, De Simone G, D'Ambrosio K (2022) α-CAs from photosynthetic organisms. Int J Mol Sci 23:12045. https://doi.org/10.3390/ijms231912045

Lazova GN, Stemler AJ (2008) A 160 kDa protein with carbonic anhydrase activity is complexed with Rubisco on the outer surface of thylakoids. Cell Biol Int 32:646–653. https://doi.org/10.1016/j.cellbi.2008.01.010

Li B, Watkinson AR (2000) Competition along a nutrient gradient: a case study with *Daucus carota* and *Chenopodium album*. Ecol Res 15:293–306. https://doi.org/10.1046/j.1440-1700.2000.00349.x

Liljas A, Kannan KK, Bergsten PC, Waara I, Fridborg K, Strandberg B et al (1972) Crystal structure of human carbonic anhydrase C. Nature New Biol 235:131–137. https://doi.org/10.1038/newbio235131a0

Lionetto MG, Caricato R, Giordano ME, Erroi E, Schettino T (2012) Carbonic anhydrase and heavy metals. In: Biochemistry. IntechOpen, pp 205–224. https://doi.org/10.5772/33372

Lionetto MG, Caricato R, Giordano ME, Schettino T (2016) Carbonic anhydrase-based biomarkers: potential application in human health and environmental sciences. Recent Pat Biomark 6:40–46. https://doi.org/10.2174/2468422806666161116143730

Lionetto MG, Caricato R, Giordano ME (2019) Pollution biomarkers in environmental and human biomonitoring. Open Biomark J 9:1–9. https://doi.org/10.2174/1875318301909010001

Makino A, Sakashita H, Hidema J, Mae T, Ojima K, Osmond B (1992) Distinctive responses of ribulose-1,5-bisphosphate carboxylase and carbonic anhydrase in wheat leaves to nitrogen nutrition and their possible relationships to CO_2-transfer resistance. Plant Physiol 100:1737–1743. https://doi.org/10.1104/pp.100.4.1737

Mandák B, Habibi F, Čortan D, Belyayev A, Jarvis DE, Jellen EN, et al. (2025)Multiple origins, singular success: genomic evidence for past recurrent hybridization in

Chenopodium album s. str. (Amaranthaceae). Mol Phylogenet Evol 215:108500. https://doi.org/10.1016/j.ympev.2025.108500

Matulis D (2016) Selective precipitation of proteins. Curr Protoc Protein Sci 83:4.5.1–4.5.37. https://doi.org/10.1002/0471140864.ps0405s83

Mohan A, Kaur R, Girdhar M (2019) Analysis of ability of *Chenopodium album* for remediation of heavy metal degraded soil. Res J Pharm Technol 12:4851–4856. https://doi.org/10.5958/0974-360X.2019.00840.0

Momayyezi M, McKown AD, Bell SC, Guy RD (2020) Emerging roles for carbonic anhydrase in mesophyll conductance and photosynthesis. Plant J 101:831–844. https://doi.org/10.1111/tpj.146381.

Mosyakin SL, Mandák B. (2020) *Chenopodium ucrainicum* (Chenopodiaceae/Amaranthaceae sensu APG), a new diploid species: a morphological description and pictorial guide. Ukr Bot J 77:237–248. https://doi.org/10.15407/ukrbotj77.04.237

Moroney JV (2026) Update: carbonic anhydrases in plants, algae, and cyanobacteria. Plant Physiol 201:kiag172. https://doi.org/10.1093/plphys/kiag172

Occhipinti R, Boron WF (2019) Role of carbonic anhydrases and inhibitors in acid–base physiology: insights from mathematical modeling. Int. J. Mol. Sci. 20(15), 3841.

Okabe K, Yang SY, Tsuzuki M, Miyachi S (1984) Carbonic anhydrase: its content in spinach leaves and its taxonomic diversity studied with anti-spinach leaf carbonic anhydrase antibody. Plant Sci Lett 33:145–153. https://doi.org/10.1016/0304-4211(84)90004-X

Ornstein L, Davis BJ (1964) Disc electrophoresis. II. Method and application to human serum protein. Ann N Y Acad Sci 121:404–427. https://doi.org/10.1111/j.1749-6632.1964.tb14213.x

Peltier J-B, Cai Y, Sun Q, Zabrouskov V, Giacomelli L, Rudella A et al (2006) The oligomeric stromal proteome of *Arabidopsis thaliana* chloroplasts. Mol Cell Proteomics 5:114–133. https://doi.org/10.1074/mcp.M500180-MCP200

Pocker Y, Ng JS (1973) Plant carbonic anhydrase: properties and carbon dioxide hydration kinetics. Biochemistry 12:5127–5134. https://doi.org/10.1021/bi00749a016

Polishchuk AV, Semenikhin AV, Topchyi NM, Zolotareva EK (2018) Inhibition of multiple forms of carbonic anhydrases of spinach chloroplasts by Cu ions. Rep Natl Acad Sci Ukr 4:94–101. https://doi.org/10.15407/dopovidi2018.04.094

Poonia A, Upadhayay A (2015) *Chenopodium album* Linn.: review of nutritive value and biological properties. J Food Sci Technol 52:3977–3985. https://doi.org/10.1007/s13197-014-1553-x

Rao MA, Scelza R, Acevedo F, Diez MC, Gianfreda L (2014) Enzymes as useful tools for environmental purposes. Chemosphere 107:145–162. https://doi.org/10.1016/j.chemosphere.2013.12.059

Rowlett RS, Chance MR, Wirt MD, Sidelinger DE, Royal J R, Woodroffe M, ... & Lam, MG (1994) Kinetic and structural characterization of spinach carbonic anhydrase. Biochemistry, 33: 13967-13976. https://doi.org/10.1021/bi00251a003

Rowlett RS (2010) Structure and catalytic mechanism of the β-carbonic anhydrases. BBA Proteins Proteom 1804:362–373. https://doi.org/10.1016/j.bbapap.2009.08.002

Rumeau D, Cuine S, Fina L, Gault N, Nicole M, Peltier G (1996) Subcellular distribution of carbonic anhydrase in *Solanum tuberosum* L. leaves: characterization of two compartment-specific isoforms. Planta 199:79–88. https://doi.org/10.1007/BF00196884

Sharma P, Tripathi S, Chandra R (2020) Phytoremediation potential of heavy metal accumulator plants for waste management in the pulp and paper industry. Heliyon 6:e04559. https://doi.org/10.1016/j.heliyon.2020.e04559

Sültemeyer D, Schmidt C, Fock HP (1993) Carbonic anhydrases in higher plants and aquatic microorganisms. Physiol Plant 88:179–190. https://doi.org/10.1111/j.1399-3054.1993.tb01776.x

Supuran CT, Scozzafava A, Casini A (2003) Carbonic anhydrase inhibitors. Med Res Rev 23:146–189. https://doi.org/10.1002/med.10025

Supuran CT (2016) Structure and function of carbonic anhydrases. Biochem J 473:2023–2032. https://doi.org/10.1042/BCJ20160115

Supuran CT (2025). Multi-and polypharmacology of carbonic anhydrase inhibitors. Pharmacol. rev., 77(1), 100004. https://doi.org/0.1124/pharmrev.124.001125

Suss KH, Arkona C, Manteuffel R, Adler K (1993) Calvin cycle multienzyme complexes are bound to chloroplast thylakoid membranes of higher plants in situ. Proc Natl Acad Sci USA 90:5514–5518. https://doi.org/10.1073/pnas.90.12.5514

Swenson ER, Maren TH (1978) A quantitative analysis of CO_2 transport at rest and during maximal exercise. Resp physiol 35(2): 129-159. https://doi.org/10.1016/0034-5687(78)90018-X

Tognacca RS, Rodríguez FS, Aballay FE, Cartagena CM, Servi L, Petrillo E (2023) Alternative splicing in plants: current knowledge and future directions for assessing the biological relevance of splice variants. J Exp Bot 74:2251–2272. https://doi.org/10.1093/jxb/erac431

Topchiy NM, Polishchuk OV, Zolotareva EK, Sytnyk SK (2019) The influence of Cd^{2+} ions on the activity of stromal carbonic anhydrases of spinach chloroplasts. Fiziol Rast Genet, 51(2):172-182. https://doi.org/10.15407/frg2019.02.172

Tőzsér D, Tóthmérész B, Harangi S, Baranyai E, Lakatos G, Fülöp Z, Simon E (2019) Remediation potential of early successional pioneer species *Chenopodium album* and *Tripleurospermum inodorum*. Nature Conservation, 36: 47-69. https://doi.org/10.3897/natureconservation.36.32503

Ugulu I, Khan ZI, Rehman S, Ahmad K, Nawaz K, Munir M, Bashir H. (2022) HeavyMetal Accumulation in Goosefoot (Chenopodiumalbum L.) Irrigated With Wastewater. Pakistan Journal of Analytical & Environmental Chemistry, 23(2): 225-236. http://doi.org/10.21743/pjaec/2022.12.05

Zhang Y, Fernie AR (2021) Metabolons, enzyme–enzyme assemblies that mediate substrate channeling, and their roles in plant metabolism. Plant Commun 2:100081. https://doi.org/10.1016/j.xplc.2020.100081

Zolotareva E, Topchiy N, Mykhaylenko N, Onoiko O (2025) Multiple forms of carbonic anhydrase in *Tetragonia tetragonioides* leaves and the impact of heavy metal ions on enzyme activity. Plant Physiol Biochem 218:109301. https://doi.org/10.1016/j.plaphy.2024.109301

Supplementary Files

This is a list of supplementary files associated with this preprint. Click to download.

- SupplementaryFile1.pdf